Effects of the Wind Speed–Evaporation–SST Feedback on the El Niño–Southern Oscillation

CHUNZAI WANG, ROBERT H. WEISBERG, AND HUIJUN YANG

Department of Marine Science, University of South Florida, St. Petersburg, Florida

(Manuscript received 3 May 1996, in final form 8 July 1998)

ABSTRACT

The thermodynamical process of latent heat flux is added to an analogical delayed oscillator model of the El Niño–Southern Oscillation (ENSO) that mainly considers equatorial ocean dynamics and produces regular, non–phase-locked oscillations. Latent heat flux affects the model sea surface temperature (SST) variations by a positive feedback between the surface wind speed and SST operating through evaporation, which is called the wind speed–evaporation–SST feedback. The wind speed–evaporation–SST feedback in which the atmosphere interacts thermodynamically with the ocean through surface heat flux differs from the conventional zonal wind stress–SST feedback in which the atmsophere interacts dynamically with the ocean through momentum flux.

The combination of equatorial ocean dynamics and thermodynamics produces relatively more realistic model oscillations. When the annual cycle amplitude of the zonal wind in the wind speed–evaporation–SST feedback is gradually increased, the model solution undergoes a transition from periodic to chaotic and then to periodic oscillations for some ranges of the parameters, whereas for other ranges of the parameters the transition goes from periodic to quasiperiodic and then to periodic oscillations. The route to chaos is the intermittency route. Along with such irregularity, the nonlinear interactions between the annual and interannual cycles operating through the wind speed–evaporation–SST feedback also produce a phase-locking of ENSO to the seasonal cycle. The model ENSO onset and peak occur in the boreal winter and spring, respectively, consistent with the observed phase-locking of ENSO in the far eastern Pacific. It is shown that ENSO decadal or interdecadal variability may result from the nonlinear interactions between the annual and interannual cycles in the Tropics.

1. Introduction

Considering the effects of equatorially trapped oceanic waves propagating in a closed basin through a delay term, Suarez and Schopf (1988) introduced the analogical delayed oscillator as a candidate mechanism for the El Niño–Southern Oscillation (ENSO). The analogical model is represented by a single ordinary differential delay equation with both positive and negative feedbacks. The positive feedback is the sum of all local processes due to the ocean–atmosphere coupling in a coupled region. The delayed negative feedback results from Kelvin waves generated at the western boundary due to the reflection of Rossby waves (Kelvin waves propagate eastward to the coupled region and reverse the anomaly pattern). Nonlinearity is also included to represent processes that limit the growth of instabilities. Based on the dynamics of the coupled ocean–atmosphere model of Zebiak and Cane (1987), Battisti and Hirst (1989) derived a version of the Suarez and Schopf (1988) analogical delayed oscillator model and showed that this delayed oscillator model could account for important aspects of the numerical coupled model. Subsequently, the oscillations found in many coupled ocean–atmosphere models of ENSO have been attributed to such delayed oscillator physics.

Although the delayed oscillator theory provides a plausible explanation for the onset, termination, and cyclic nature of ENSO events, it fails to explain two basic ENSO characteristics as observed in nature. First, ENSO events, which occur roughly twice per decade, are irregular. Second, ENSO exhibits a strong tendency for phase-locking to the seasonal cycle in the sense that maximum sea surface temperature (SST) anomalies occur during a particular calendar month. For example, Rasmusson and Carpenter (1982) showed that in the far eastern Pacific (between 95° and 80°W) the onset of El Niño occurs around Christmastime and the peak phase of El Niño is in late boreal spring of the El Niño year, whereas in the Nino3 region (5°S–5°N, 150°–90°W) the onset is in boreal spring and the peak is near the end of the El Niño year (December). Recently, B. Wang (1995) further showed that the peak phases of El Niño in the far eastern Pacific are different during the pre-1977 and the post-1977 warm episodes. The far eastern

Corresponding author address: Dr. Chunzai Wang, Physical Oceanography Division, NOAA/Atlantic Oceanographic and Meteorological Laboratory, 4301 Rickenbacker Causeway, Miami, FL 33149.

Pacific peak phase of El Niño in the pre-1977 warm episodes occurs in late boreal spring of the El Niño year, whereas the peak phase in the post-1977 warm episodes is in boreal spring of the subsequent year of the El Niño year. Motivated by the inconsistencies of the theory with observations, this paper attempts to improve upon the delayed oscillator theory by considering an additional physical process.

There have been several hypotheses on the irregularity of ENSO. One class of these considers interactions between the annual and interannual cycles. For example, Jin et al. (1994), Tziperman et al. (1994), Tziperman et al. (1995), and Chang et al. (1994, 1995) use different numerical coupled ocean–atmosphere models to argue that annual forcing is responsible for the irregularity of model ENSO events. They claimed that the model ENSO can be explained as a low-order chaotic behavior driven by the annual cycle and the chaotic oscillations are created by nonlinear resonance between the annual and interannual cycles. The routes to chaos in different model are different. The transition to chaos in the model of Chang et al. (1995) follows the period-doubling route. Tziperman et al. (1995) demonstrated that as either the coupling strength or the amplitude of the background seasonal cycle in the model of Zebiak and Cane (1987) is increased, the model undergoes a transition from periodic to chaotic behavior according to the universal quasiperiodicity route to chaos. However, they did not identify which of the physical processes is the major cause of the nonlinear resonances and, therefore, of the model chaotic behavior.

The present study examines whether a delayed oscillator model will produce irregular oscillations and phase-locking if additional physics is considered. The delayed oscillator model mainly emphasized equatorial ocean dynamics. The thermodynamics of surface heat flux as a whole is simplistically treated as a Newtonian cooling included in the local coupling process term. Such a simplistic treatment suppresses the positive feedback between surface wind speed and SST operating through an evaporation process, which is called the wind speed–evaporation–SST feedback. The feedback, in which surface wind through surface heat flux affects SST, which in turn affects surface wind, can be described as follows. In response to increasing (decreasing) surface wind speed, evaporation is increased (decreased). Increasing (decreasing) evaporation results in more (less) SST cooling, which in turn further increases (decreases) the surface wind speed. This wind speed–evaporation–SST feedback is important in controlling the latitudinal climate asymmetry related to the intertropical convergence zone (ITCZ) in the eastern Pacific (e.g., Xie and Philander 1994; Xie 1996). Observations have also pointed out the importance of the wind speed–evaporation–SST feedback in the equatorial Pacific (C. Wang 1995; Weisberg and Wang 1997). The positive wind speed–evaporation–SST feedback is physically different from the conventional zonal wind stress–SST feedback [see Philander (1990) and McCreary and Anderson (1991) for a review], which emphasizes the ocean and atmosphere interactions through momentum flux. In this paper, we will investigate how the periodic solutions of the delayed oscillator model transform into aperiodic (or chaotic) solutions and how the model oscillations are phase-locked to the seasonal cycle by adding the wind speed–evaporation–SST feedback. The paper also discusses the possibility of the nonlinear interactions between the annual and interannual cycles inducing lower-frequency (decadal or interdecadal) climate variability.

The paper is organized as follows. Section 2 reviews the behaviors of the conventional delayed oscillator model, and presents the physics of the modified delayed oscillator model in which the wind speed–evaporation–SST feedback process is added. Section 3 introduces the results of the irregularity and phase-locking of the model oscilllations due to the wind speed–evaporation–SST feedback process. Section 4 summarizes and discusses the results.

2. Conceptual oscillation models

Before the wind speed–evaporation–SST feedback is considered, we first review the conventional delayed oscillator.

a. The delayed oscillator model

The nonlinear delayed oscillator equation was first proposed by Suarez and Schopf (1988) as an analogical model of the ENSO phenomenon. Battisti and Hirst (1989) then derived the version of the Suarez and Schopf (1988) delayed oscillator model that was specifically designed to contain the important dynamics of the coupled ocean–atmosphere model of Zebiak and Cane (1987). The analogical model is represented by an ordinary differential delay equation,

$$\frac{dT}{dt} = aT - bT(t - \tau) - eT^3. \tag{1}$$

The first term on the right-hand side of Eq. (1) summarizes all the processes that include local change of the SST anomaly T. Note that Newtonian cooling parameterized as a constant coefficient is also included in this local coupling term [see Battisti and Hirst (1989) for details]. The second term represents the delayed negative feedback effect on T of Rossby waves that are excited in a coupled region and later reflected from the western boundary as equatorial Kelvin waves with delay time τ. The third cubic term represents processes that limit the growth of instabilities.

The nature of the solutions to Eq. (1) depends upon the values of the coefficients a, b, e, and τ, allowing either steady or oscillatory solutions. For a steady state ($dT/dt = 0$), it follows that when $a > b$ the system has

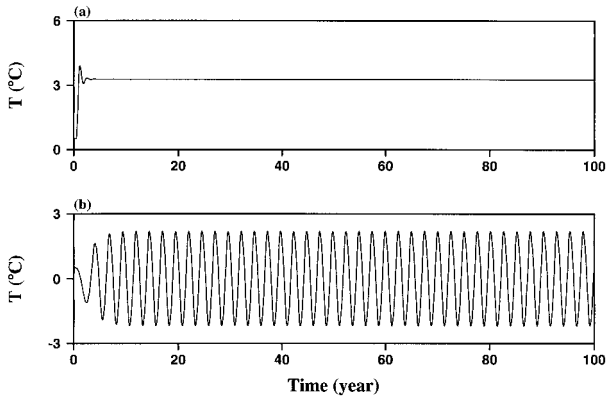

FIG. 1. Solutions of the conventional delayed oscillator model [Eq. (1)]. The model parameters are (a) $a = 6.8\ \text{yr}^{-1}$, $b = 2.5\ \text{yr}^{-1}$, $e = 0.4\ ^\circ\text{C}^{-2}\ \text{yr}^{-1}$, $\tau = 0.5$ yr; and (b) $a = 2.3\ \text{yr}^{-1}$, $b = 2.7\ \text{yr}^{-1}$, $e = 0.4\ ^\circ\text{C}^{-2}\ \text{yr}^{-1}$, $\tau = 0.5$ yr.

three steady solutions: an inner solution $T = 0$; and two outer symmetric solutions

$$T = \pm T_E = \pm\left(\frac{a - b}{e}\right)^{1/2}, \qquad (2)$$

which represent the permanent El Niño and La Niña states, respectively. However, when $a < b$ there are no permanent El Niño and La Niña outer states. The system has only one steady real solution, $T = 0$.

Different authors have used different model parameter ranges of Eq. (1), claimed to be relevant to particular coupled ocean–atmosphere models. McCreary and Anderson (1991) summarized and presented the parameter dependence on the solutions of Eq. (1). Since the purpose of this paper is to examine whether the inclusion of the wind speed–evaporation–SST feedback in the delayed oscillator can transform periodic solutions to chaotic oscillations and whether the modified delayed oscillator can produce phase-locking of ENSO to the seasonal cycle, model parameters a, b, e, and τ are used without constraints to any particular coupled ocean–atmosphere models. In this paper, two sets of model parameters (which fall in model parameter ranges $a > b$ and $a < b$) are considered to demonstrate the effect of the wind speed–evaporation–SST feedback.

The ordinary differential Eq. (1) is integrated by the predictor–corrector method of the Adams–Bashforth–Moulton scheme. The time evolutions of typical solutions of Eq. (1) are shown in Figs. 1a and 1b with two sets of the model parameters: $a = 6.8\ \text{yr}^{-1}$, $b = 2.5\ \text{yr}^{-1}$, $e = 0.4\ ^\circ\text{C}^{-2}\ \text{yr}^{-1}$, $\tau = 0.5$ yr; and $a = 2.3\ \text{yr}^{-1}$, $b = 2.7\ \text{yr}^{-1}$, $e = 0.4\ ^\circ\text{C}^{-2}\ \text{yr}^{-1}$, $\tau = 0.5$ yr. The system for the first set of model parameters ($a > b$) does not oscillate, with the solution converging quickly to the permanent El Niño state (Fig. 1a). This corresponds to a case in which the delayed negative feedback effect is not strong enough to switch the permanent El Niño state to the La Niña state (or La Niña state to El Niño state, depending on the initial condition). The solution for the second set of model parameters ($a < b$) is perfectly periodic with a period about 2.5 yr (Fig. 1b). There are no permanent El Niño or La Niña states in this model parameter range. The system oscillates about a single, unstable zero basic state ($T = 0$).

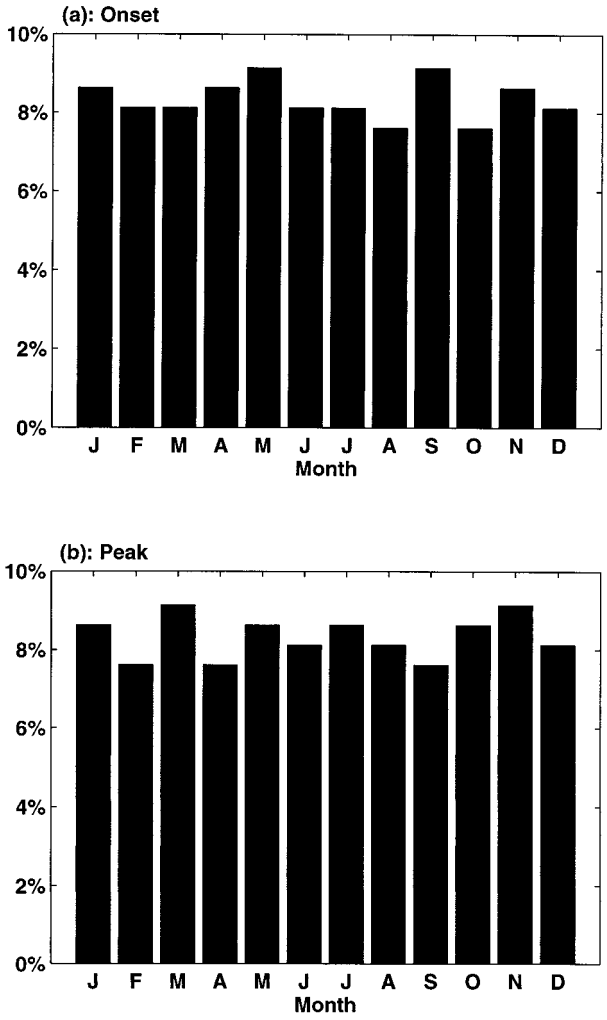

FIG. 2. Histograms of the percentage for (a) model ENSO onset and (b) model ENSO peak as a function of calendar month. The model corresponding to Fig. 1b was integrated for 500 yr, and then the months of the model ENSO onset and peak were tabulated.

In order to examine the phase-locking of the delayed oscillator, Eq. (1) with the second set of model parameters of Fig. 1b was integrated for 500 years. We then tabulated months of model ENSO onset (defined by SST anomaly becoming positive) and model ENSO peak. Histograms of the percentage for model ENSO onset and model ENSO peak as a function of calendar month are shown in Figs. 2a and 2b, respectively. Both the model ENSO onset and peak occur over all calendar months. The model ENSO is not phase-locked to the seasonal cycle, contrary to observations that the onset

and peak phases of ENSO are phase-locked to particular months (e.g., Rasmusson and Carpenter 1982; B. Wang 1995). This absence of irregularity and phase-locking to the seasonal cycle suggests that some essential physics are omitted in this analogical delayed oscillator model.

b. *Effect of latent heat flux on a delayed oscillator model*

In some numerical models, surface heat fluxes as a whole have been simplistically treated as Newtonian cooling using a temporally constant coefficient. For example, Oberhuber (1988) demonstrated how the heat flux could be simplified as a Newtonian cooling or the heat flux correction term in simulating SST in an ocean general circulation model. Letting an overbar denote the temporal mean and a prime denote the deviation (or anomaly) from the mean, the surface heat flux anomaly Q' can be expressed as

$$Q' = Q - \overline{Q} = \left.\frac{\partial Q}{\partial T}\right|_{T=\overline{T}} (T - \overline{T}) = -\alpha T', \quad (3)$$

where $\alpha \equiv -(\partial Q/\partial T)|_{T=\overline{T}} =$ constant is the coefficient of Newtonian cooling. This simple Newtonian cooling term was included in the local coupling feedback term aT in the conventional delayed oscillator of Eq. (1) (Battisti and Hirst 1989).

The above treatment of surface heat flux, however, does not consider the feedback between surface wind speed and SST operating through evaporation. Treating surface heat fluxes as a simple Newtonian cooling suppresses the active wind speed–evaporation–SST feedback. Increasing surface wind speed enhances surface evaporation (latent heat flux) and thus cools SST, which further increases surface wind speed. In order to consider the wind speed–evaporation–SST feedback in the model, we divide the total surface heat flux Q into the latent heat flux Q_{Lat} and other surface heat fluxes Q_{Other}. Thus, the surface heat flux anomaly Q' is

$$\begin{aligned} Q' &= Q - \overline{Q} = Q_{\text{Other}} - \overline{Q}_{\text{Other}} - (Q_{\text{Lat}} - \overline{Q}_{\text{Lat}}) \\ &= \left.\frac{\partial Q_{\text{Other}}}{\partial T}\right|_{T=\overline{T}} (T - \overline{T}) - \left.\frac{\partial Q_{\text{Lat}}}{\partial T}\right|_{T=\overline{T}} (T - \overline{T}) \\ &= -\alpha_N T' - \rho_a L C_E \left.\left(\frac{\partial q_s}{\partial T}\right)\right|_{T=\overline{T}} U_a T', \end{aligned} \quad (4)$$

where $\alpha_N \equiv -(\partial Q_{\text{Other}}/\partial T)|_{T=\overline{T}}$, ρ_a is the air density, L is the latent heat of vaporation, C_E is the exchange coefficient, the saturated moisture content q_s is given by the Clausius–Clapeyron equation, and U_a is the surface wind speed.

In addition to the Newtonian cooling term $\alpha_N T'$, which parameterizes surface insolation, longwave radiation, and sensible heat flux, there is another term in Eq. (4) that paramaterizes latent heat flux and is proportional to the product of SST anomaly T' and surface wind speed U_a. Using this treatment of the surface heat flux as shown in Eq. (4) and dropping the prime for clarity, a modified delayed oscillator model can be written as

$$\frac{dT}{dt} = aT - bT(t - \tau) - eT^3 - c|\overline{U} + U|T, \quad (5)$$

where $\overline{U}$ is the mean zonal wind, U is the zonal wind anomaly, $c = \rho_a L C_E (\partial q_s/\partial T)|_{T=\overline{T}} (\rho c_p h)^{-1}$, ρ is the density of sea water, c_p is the heat capacity of seawater at constant pressure, and h is the mixed layer depth. With $\overline{T} = 301$ K and h varying from 50 to 150 m, the parameter c related to the wind speed–evaporation–SST feedback ranges between 0.8 and 0.2 s m^{-1} yr^{-1}. Note that the meridional wind has been neglected in calculating the wind speed for simplicity. The last term on the right-hand side of Eq. (5) represents the process of latent heat flux, acting as a cooling effect on SST anomaly ($c > 0$). Unlike conventional treatment of latent heat flux as a Newtonian cooling, it also depends upon the surface wind speed. It is the dependence upon the surface wind speed that forms a positive wind speed–evaporation–SST feedback. Physically, in response to a decrease (increase) in SST, the surface wind speed is strengthened (weakened). The strengthening (weakening) of the surface wind speed increases (decreases) the latent heat flux, which, in turn, results in more (less) SST cooling. The wind speed–evaporation–SST feedback in which the atmosphere interacts thermodynamically with the ocean through surface heat flux differs from the conventional zonal wind stress–SST feedback in which the atmsophere interacts dynamically with the ocean through momentum flux. Further discussion and comparisons of these two feedbacks are given in section 4.

Equation (5) has two unknowns, T and U. To get a closed form, we need another equation controlling the variation of U. It is observed that zonal wind anomaly is highly correlated with SST anomaly in the equatorial Pacific (e.g., Hayes et al. 1991; Latif and Barnett 1995). Thus, we assume that

$$\frac{dU}{dt} = fT - gU, \quad (6)$$

where f is a forcing parameter and g is a damping coefficient, and their values are positive, representing the observed relation between zonal wind and SST anomalies. Equation (6) states that zonal wind U tends to adjust to be linearly related to T. A similar relationship to Eq. (6) was used by Graham and White (1988) who assumed that the time derivative of zonal wind stress anomaly in the central equatorial Pacific is proportional to SST anomaly in the eastern equatorial Pacific. In an overview of coupled ocean–atmosphere models of ENSO, McCreary and Anderson (1991) further commented on Eq. (6) as being the relationship that

models Bjerknes's Walker circulation. For further simplification, the time derivative in Eq. (6) can be dropped (a steady atmosphere).

Similar to the steady and symmetric solutions of Eq. (2), we can analyze the steady solutions of Eqs. (5) and (6). In this case the solutions, which depend upon the mean zonal wind $\overline{U}$ relative to the steady state of zonal wind U_E, are

$$T = T_E = \begin{cases} \dfrac{1}{2ge}\{cf \pm [c^2f^2 - 4g^2e(-c\overline{U} + b - a)]^{1/2}\}, & \text{if } -\overline{U} \geq U_E = \dfrac{f}{g}T_E; \\ \dfrac{1}{2ge}\{-cf \pm [c^2f^2 - 4g^2e(c\overline{U} + b - a)]^{1/2}\}, & \text{if } -\overline{U} < U_E = \dfrac{f}{g}T_E. \end{cases} \tag{7}$$

Unlike the symmetric solutions of Eq. (2), the solutions of Eq. (7) are asymmetric. That is, the amplitudes of the permanent El Niño and La Niña states are unequal and vary with the model parameters.

Observations show that in the eastern equatorial Pacific surface wind has a large annual cycle (e.g., Hayes et al. 1991). The easterly trade wind is weakest in the boreal spring whereas it is strongest in the boreal fall. Therefore, when the wind speed–evaporation–SST feedback is considered, the realistic mean zonal wind should have an annual cycle. To account for the annual cycle, the mean zonal wind in Eq. (5) is specified as

$$\overline{U} = U_0 + U_1 \sin(\omega t), \tag{8}$$

where U_0 is a constant parameter, U_1 is the amplitude of the annual cycle, and $\omega = 2\pi$ yr^{-1} is the annual frequency. In the subsequent experiments, the clock is set so that the weakest (strongest) mean zonal wind occurs in the boreal spring (fall), consistent with observations.

3. Main results

In a similar manner as the integration of Eq. (1), Eqs. (5) and (6) were integrated by the predictor-corrector method of the Adams–Bashforth–Moulton scheme. The modified delayed oscillator model of Eqs. (5) and (6) has nine parameters and its behavior depends upon these model parameters. The purpose of this paper is to examine how the wind speed–evaporation–SST feedback transforms the periodic model ENSO solution into an irregular solution and how this feedback introduces the phase-locking of ENSO to the seasonal cycle. Therefore, we fixed all other model parameters and took the annual cycle amplitude of the mean zonal wind $\overline{U}$ in the wind speed–evaporation–SST feedback process as a varying parameter. The range of this varying parameter U_1 is chosen to be physically reasonable based on observations. The two previous sets of model parameters, representing the permanent El Niño steady solution and periodic solution of the delayed oscillator Eq. (1) as shown in Figs. 1a and 1b, are used to demonstrate how the wind speed–evaporation–SST feedback modifies the solutions.

a. Chaotic oscillations

The first set of the model parameters is $a = 6.8$ yr^{-1}, $b = 2.5$ yr^{-1}, $e = 0.4$ °C^{-2} yr^{-1}, $\tau = 0.5$ yr, $c = 0.6$ s m^{-1} yr^{-1}, $U_0 = -4.0$ m s^{-1}, $f = 6.0$ m s^{-1} °C^{-1} yr^{-1}, and $g = 18.0$ yr^{-1}. The time evolutions of SST anomaly T for different U_1 are shown in Figs. 3a–e. Note that the time series of the zonal wind anomaly U are not shown since they are similar to T. When U_1 is weak, the permanent El Niño (or La Niña, depending on the initial condition) state is replaced by the oscillatory state around the permanent state. With $U_1 = 1.0$ m s^{-1}, the time series of model T shows small oscillations about an El Niño state (or La Niña state) with an annual period (Fig. 3a). When U_1 is increased to above 2.5 m s^{-1}, the model starts to oscillate between the El Niño and La Niña states irregularly, favoring the El Niño state (see Fig. 3b for $U_1 = 2.8$ m s^{-1}). Further increase in U_1 produces more chaotic oscillations between the El Niño and La Niña states (Figs. 3c and 3d). However, when U_1 is increased above 4.4 m s^{-1}, the periodic solution appears, oscillating between the two states with a period of 2 yr (see Fig. 3e for $U_1 = 5.0$ m s^{-1}). Thus, for this set of the model parameters, in which the delayed negative feedback effect alone is not enough to switch the El Niño state into the La Niña state or vice versa (see Fig. 1a), the wind speed–evaporation–SST feedback helps the system to oscillate between the permanent El Niño and La Niña states. As the annual cycle amplitude of mean zonal wind is gradually increased, the solution undergoes the transition first from the oscillatory El Niño state to chaotic oscillations, and then to periodic oscillations between the El Niño state and La Niña state.

The evolution of the system can be better described in phase space in terms of dynamical system theory. The phase space is reconstructed by using the method of delay coordinates. Figures 4a–e show phase space diagrams corresponding to the time series in Figs. 3a–e. For example, the periodic solution in the time series

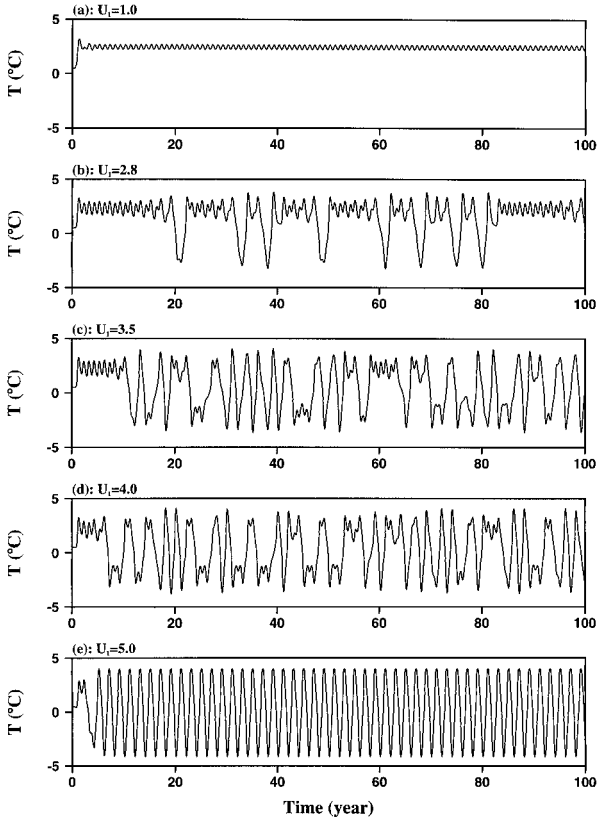

FIG. 3. The time evolutions of SST anomaly for different annual cycle amplitudes of zonal wind U_1: (a) U_1 = 1.0 m s^{-1}; (b) U_1 = 2.8 m s^{-1}; (c) U_1 = 3.5 m s^{-1}; (d) U_1 = 4.0 m s^{-1}; (e) U_1 = 5.0 m s^{-1}. Other model parameters are given in the text.

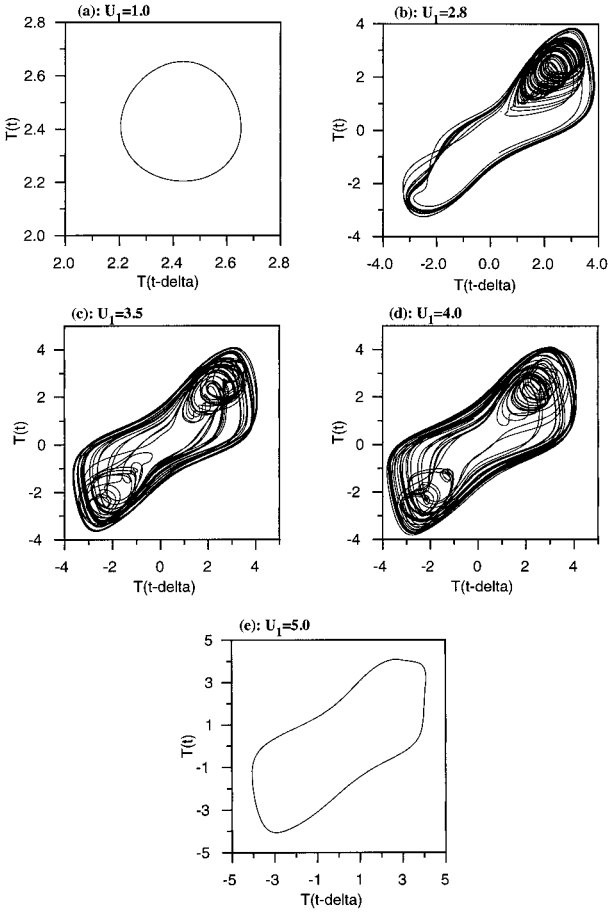

FIG. 4. Phase space diagrams of the model solutions corresponding to Figs. 3a–e. The phase space is reconstructed by using the method of delay coordinates. The delay parameter delta is chosen with 6 months.

(Figs. 3a and 3e) corresponds to a closed cycle in the phase space (Figs. 4a and 4e). There is an attractor when the solution oscillates irregularly (Figs. 4b–d, corresponding to the time series in Figs. 3b–d). When U_1 is relatively weak the trajectory is mostly attracted into the El Niño center (see Fig. 4b). However, when U_1 is further increased the attractor has two centers, corresponding to the El Niño and La Niña states. The trajectory will stay in the El Niño center for a while, then spirals out to the La Niña center, and later spirals back to the El Niño center. This behavior is very similar to that of the Lorenz system (Lorenz 1963). For this set of the parameters, like the Lorenz system our system is indeed a strong dissipative system due to strong dissipation in the SST and zonal wind perturbation [Eqs. (5) and (6)]. Such dynamical behavior also can be quantified by the Lyapunov exponent, which describes the exponential rate of divergence of the trajectories in phase space. A positive Lyapunov exponent indicates chaotic behavior (Guckenheimer and Holmes 1983). There are several methods for calculating the exponent. Here we employed the delay coordinate method (Guckenheimer and Holmes 1983; Wolf et al. 1985). The results show that as U_1 increases from 2.8 to 4.0 m s^{-1}, the Lyapunov exponent also increases and the system becomes more chaotic as discussed previously. For example, for the cases of U_1 = 2.8, 3.5, and 4.0 m s^{-1} the Lyapunov exponent is 0.104, 0.140, and 0.183 yr^{-1}, respectively.

The transition to chaos of a model system can occur in one of three universally recognized standard scenarios: the period-doubling route, the quasiperiodicity route, and the intermittency route (Guckenheimer and Holmes 1983). Each of these routes has different and unique properties. The first two routes of transition to chaos have been identified in ENSO models. For example, Chang et al. (1995) showed the period-doubling route and Tziperman et al. (1995) demonstrated the quasiperiodicity route. The transition to chaos in the present system takes the third route, that of the intermittency route.

In the intermittency transition to a chaotic attractor the following phenomena take place. For values of the system parameter (such as U_1) less than a critical transition value (U_{1c}), the attractor is a periodic orbit. For U_1 slighly larger than U_{1c} there are long stretches of

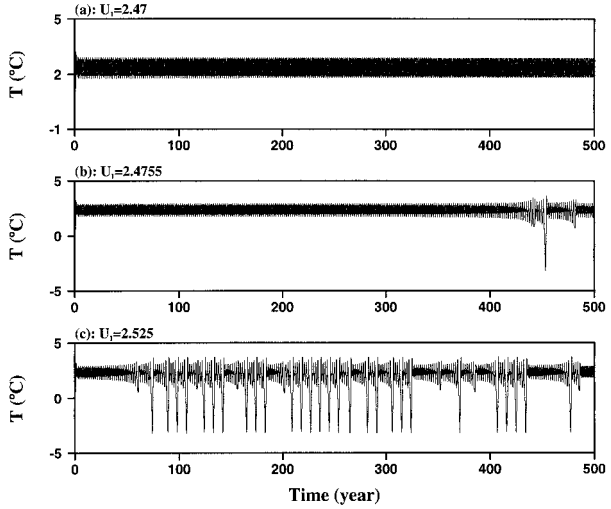

FIG. 5. The time evolutions of SST anomaly shown the model transition from periodicity to chaos in Fig. 3: (a) $U_1 = 2.47$ m s^{-1}; (b) $U_1 = 2.4755$ m s^{-1}; (c) $U_1 = 2.525$ m s^{-1}.

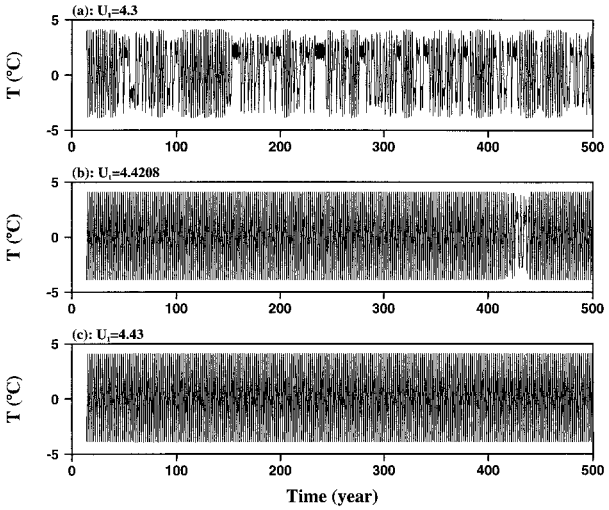

FIG. 6. The time evolutions of SST anomaly showing the model transition from chaos to periodicity in Fig. 3: (a) $U_1 = 4.3$ m s^{-1}; (b) $U_1 = 4.4208$ m s^{-1}; (c) $U_1 = 4.43$ m s^{-1}.

time during which the orbit appears to be periodic and closely resembles the orbit for $U_1 < U_{1c}$, but this regular (approximately periodic) behavior is intermittently interrupted by a finite duration ''burst'' in which the orbit behaves in a decidely different manner. These bursts occur at seemingly random times, but one can define a mean time between the bursts. As the parameter approaches the critical value from above, the mean time between bursts approaches infinity and the attractor orbit thus becomes always ''laminar'' so that the oscillation is periodic. As the parameter increases substantially above the critical value, U_{1c}, the bursts become so frequent that the regular oscillation can no longer be distinguished. The present system illustrates this transition very well, as shown in Fig. 5. The smaller value $U_1 = 2.47$ m s^{-1} corresponds to stable periodic oscillation (Fig. 5a). As U_1 is increased to 2.4755 m s^{-1}, there appears one burst after almost 450 yr (Fig. 5b). Before the first burst occurs, the oscillation appears almost periodic (laminar phase). As U_1 is further increased the bursts become much more frequent as shown in Fig. 5c. Thus, the critical value is $U_{1c} = 2.4755$ m s^{-1}. The transition from chaos to periodic oscillations is through the same route but in reverse order, as shown in Fig. 6 with the critical value of $U_{1c} = 4.4208$ m s^{-1}. The smaller value corresponds to a chaotic attractor (Fig. 6a). As the parameter is increased, the oscillation appears almost periodic during the first 400 yr and then one burst occurs and again the oscillation becomes almost periodic in the following long time (Fig. 6b). As U_1 is further increased, the oscillation becomes periodic (Fig. 6c).

In order to examine the phase-locking of ENSO to the seasonal cycle, the model was integrated for 500 yr with parameters as in Fig. 3d. The months of model ENSO onset and model ENSO peak were then tabulated. Histograms of the percentage for model ENSO onset and model ENSO peak as a function of calendar month are shown in Figs. 7a and 7b, respectively. The model ENSO onset occurs during the boreal winter whereas the model ENSO peak occurs during the boreal spring. The model ENSO is phase-locked to the seasonal cycle, consistent with observations in the far eastern Pacific. While not shown, all other cases with different values of U_1 in Fig. 3 also display the phase-locking to the seasonal cycle. The phase-locking of ENSO in this model is caused by the positive wind speed–evaporation–SST feedback in which the annual cycle of mean zonal wind is specified to be consistent with observation in that the easterly wind is weakest (strongest) in the boreal spring (fall).

b. Quasiperiodic oscillations

The second set of the model parameters is $a = 2.3$ yr^{-1}, $b = 2.7$ yr^{-1}, $e = 0.4$ °C^{-2} yr^{-1}, $\tau = 0.5$ yr, $c = 0.3$ s m^{-1} yr^{-1}, $U_0 = -4.0$ m s^{-1}, $f = 6.0$ m s^{-1} °C^{-1} yr^{-1}, and $g = 18.0$ yr^{-1}. The time evolutions of SST anomaly for different U_1 are shown in Figs. 8a–e. For this set of the model parameters, in which the conventional delayed negative feedback effect is able to make the system oscillate (see Fig. 1b), the wind speed–evaporation–SST feedback also modifies the solutions. When U_1 is very small, the solution of Eqs. (5) and (6) exhibits an almost periodic oscillation between the El Niño and La Niña state with a period of 2.4 yr (Fig. 8a). As U_1 is increased, the oscillation becomes quasi-periodic (Fig. 8b). As U_1 is further increased, the oscillation appears almost irregular (Fig. 8c), but not chaotic (to be discussed shortly using spectral analyses). However, as U_1 is further increased, the oscillation again becomes quasiperiodic (Fig. 8d). Periodic oscillations appear when U_1 is increased further (Fig. 8e).

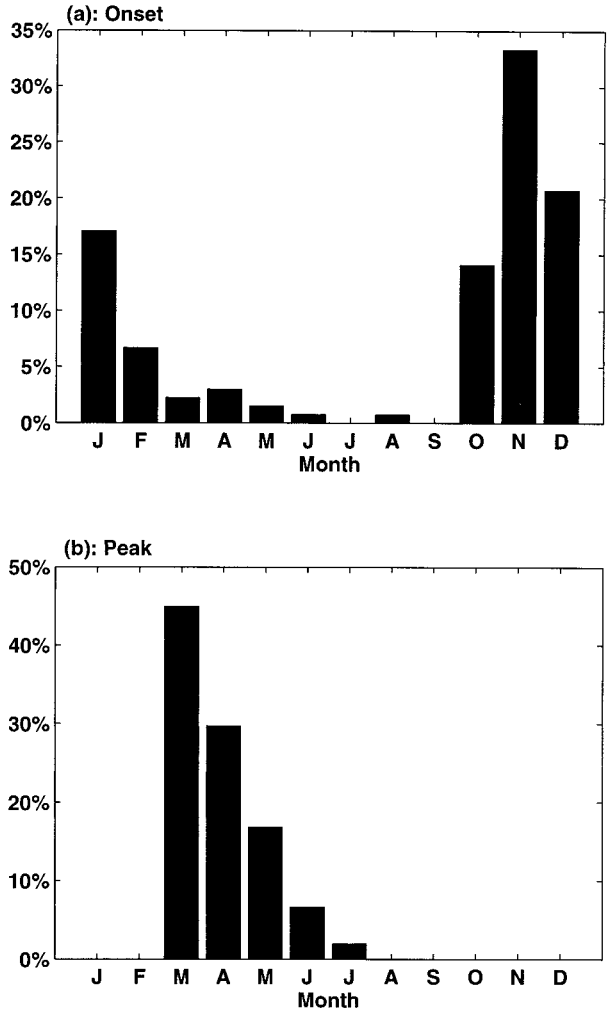

FIG. 7. Histograms of the percentage for (a) model ENSO onset and (b) model ENSO peak as a function of calendar month. The model corresponding to Fig. 3d was integrated for 500 yr, and then the months of the model ENSO onset and peak were tabulated.

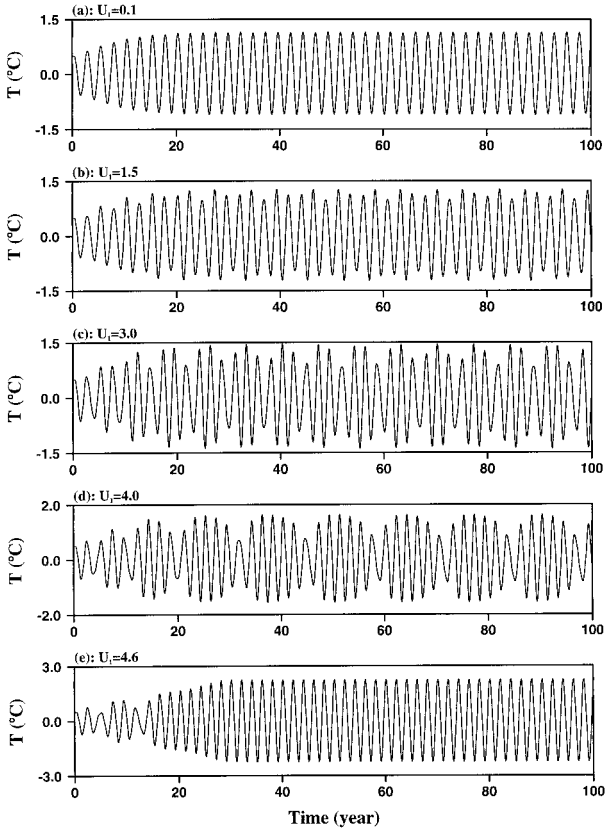

FIG. 8. The time evolutions of SST anomaly for different annual cycle amplitudes of zonal wind U_1: (a) $U_1 = 0.1$ m s^{-1}; (b) $U_1 = 1.5$ m s^{-1}; (c) $U_1 = 3.0$ m s^{-1}; (d) $U_1 = 4.0$ m s^{-1}; (e) $U_1 = 4.6$ m s^{-1}. Other model parameters are given in the text.

Corresponding trajectories in phase space and spectral analyses are shown in Figs. 9 and 10, respectively. Again the closed cycles (Figs. 9a and 9e) are found for the periodic (or almost periodic) solutions (Figs. 8a and 8e). However, there are several distinctions between this set of the model parameters and the previous one. First, when U_1 is weak the solution oscillates between the El Niño and La Niña states, whereas in the previous set of the parameters it oscillates around the El Niño state. Second, there is lack of two attractor centers for this set of the parameters. Third, the phase space suggests that the model solutions are not chaotic although Fig. 9c shows a more complex phase space. Whether or not the model solutions for this set of the parameters is chaotic may be addressed by spectral analyses. In the nonchaotic regime the autospectrum is normally characterized by several very sharp peaks, whereas in the chaotic regime the spectral peaks become fewer and broader. Figure 10e shows that when the model solution is simply periodic, there is only one peak in the autospectrum. In other cases the autospectrum has a sharp main peak and many sharp subpeaks. With this kind of spectral behavior, the model oscillation is called quasiperiodicity (Guckenheimer and Holmes 1983). The almost irregular oscillation of Fig. 10c is, in fact, a complex quasiperiodicity oscillation, but not chaotic since the autospectrum still shows sharp peaks without broad spectrum.

The phase-locking of the model ENSO to the seasonal cycle in this set of the parameters is also studied by running the model for 500 yr. As an example, with the model parameters of Fig. 8c the histograms of the percentage for model ENSO onset and model ENSO peak as a function of calendar month are shown in Figs. 11a and 11b, respectively. The model ENSO is also phase-locked to the seasonal cycle. The model ENSO onset occurs during the boreal winter and the model ENSO peak warm phase occurs during the late boreal spring. For this set of the model parameters, only the $U_1 = 0.1$ m s^{-1} case does not show the phase-locking because of a very weak annual cycle in this case. This suggests

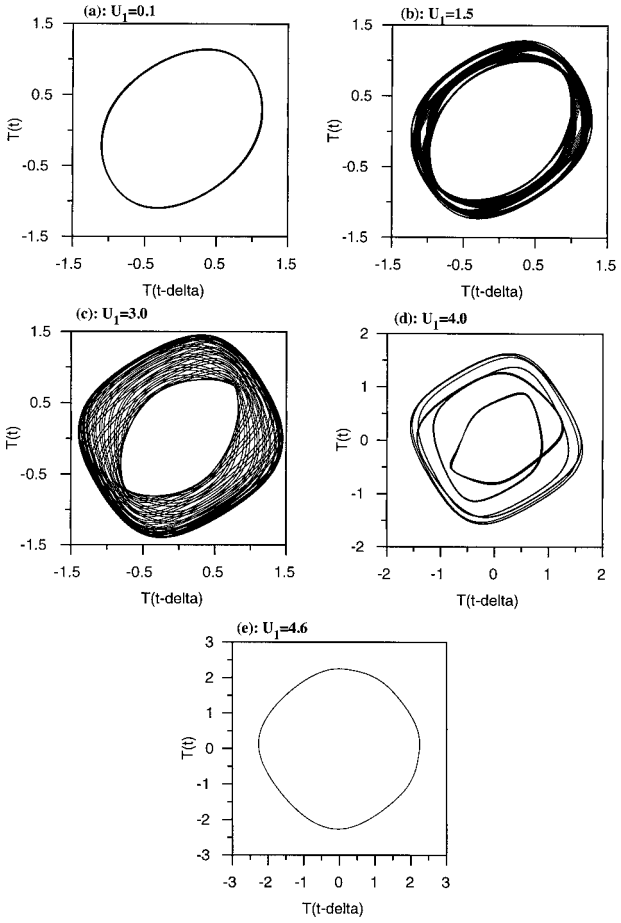

FIG. 9. Phase space diagrams of the model solutions corresponding to Figs. 8a–e. The phase space is reconstructed by using the method of delay coordinates. The delay parameter delta is chosen with 3 months.

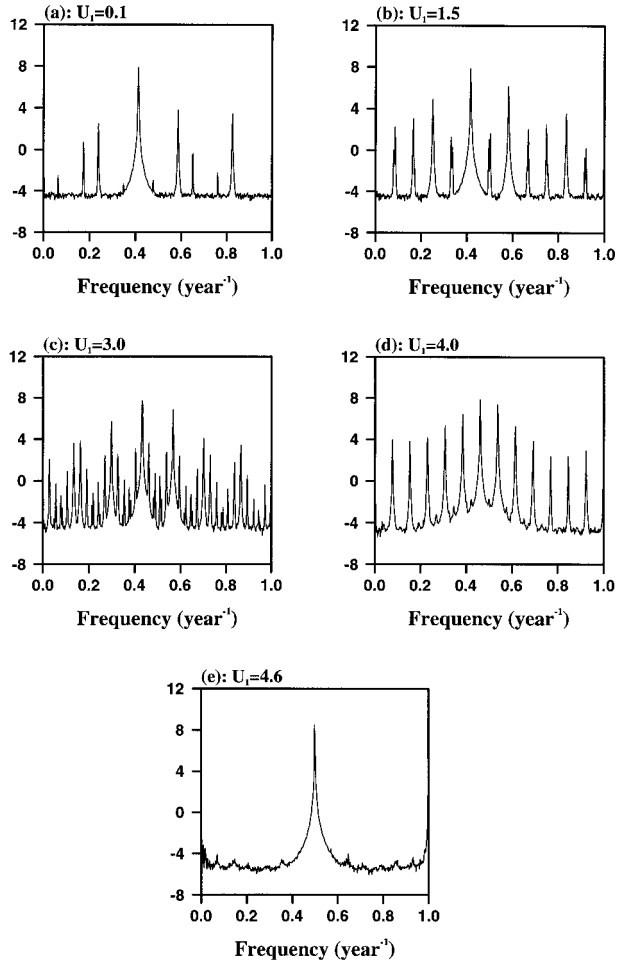

FIG. 10. Logarithm of autospectrum for model time series. The model corresponding to Figs. 8a–e was integrated for 4000 yr, then the output of SST anoamly was used to calculate the autospectrum.

that the annual cycle in mean zonal wind is the key for phase-locking of ENSO to the seasonal cycle.

There is decadal variability in Fig. 8d in addtion to interannual variability. This suggests that the nonlinear interactions between the annual and interannual cycles can produce lower-frequency oscillations. A physical explanation may follow from wave packet theory (Guckenheimer and Holmes 1983). In a linear system, the summation of two high-frequency oscillations will produce a lower-frequency oscillation that is called a wave packet. The frequency of the wave packet is the frequency difference between high frequencies. In a nonlinear system, the resulting lower-frequency oscillations are further modulated by nonlinearity. The model SST decadal variability in Fig. 8d resembles a wave packet.

4. Summary and discussion

The conventional delayed oscillator, which mainly considers equatorial ocean dynamics, provides an explanation for the onset, termination, and cyclic nature of ENSO. However, it fails to explain the irregularity of ENSO and the phase-locking of ENSO to the seasonal cycle as observed in nature. Motivated by these inconsistencies with observations, thermodynamics of the latent heat flux process is added to the delayed oscillator model. This additional process, depending upon the feedback between the surface wind speed and SST operating through evaporation, modifies the oscillatory behaviors of the conventional delayed oscillator model. When the annual cycle amplitude of mean zonal wind in the wind speed–evaporation–SST feedback is gradually increased, for some ranges of the parameters the model undergoes the transition from periodic to chaotic and then to periodic oscillations, whereas for other ranges of the parameters the transition of the model solutions goes from periodic to quasiperiodic and then back to periodic. The route to chaos is the intermittency route. The realistic annual cycle of zonal wind in the far eastern Pacific produces the phase-locking of ENSO to the

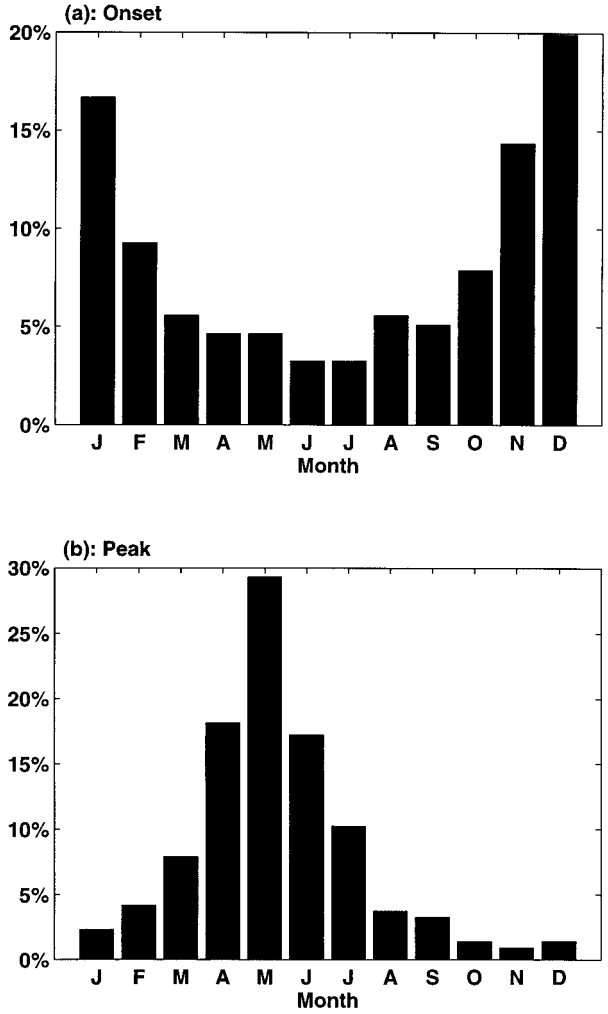

FIG. 11. Histograms of the percentage for (a) model ENSO onset and (b) model ENSO peak as a function of calendar month. The model corresponding to Fig. 8c was integrated for 500 yr, and then the months of the model ENSO onset and peak were tabulated.

seasonal cycle over there. This simple model also produces lower-frequency oscillations, suggesting that decadal or interdecadal variability may result from the nonlinear interactions between the annual and interannual cycles in the Tropics. In terms of an analogical delayed oscillator model, the paper demonstrates that both equatorial ocean dynamics and thermodynamics, which occur on different timescales, are necessary for aperiodic oscillations.

The thermodynamics affects the oscillatory behaviors of the delayed oscillator model through the positive wind speed–evaporation–SST feedback. This feedback is physically different from the conventional positive zonal wind stress–SST feedback (e.g., Philander 1990; McCreary and Anderson 1991) of a coupled tropical ocean–atmosphere system in that the atmosphere interacts thermodynamically with the ocean through surface heat flux. C. Wang (1995) and Weisberg and Wang (1997) found that the wind speed–evaporation–SST feedback is important on seasonal and intraseasonal timescales, based on in situ observations. The positive wind speed–evaporation–SST feedback, in which surface wind speed through evaporation affects SST, which in turn affects wind speed, can be explained as follows. In response to an increase in SST, the atmosphere shows an increase in cumulus convection and moisture content difference. Convection induces surface wind convergence that lowers wind speed at its center thereby tending to decrease the heat flux. On the other hand, the increase in moisture content difference tends to increase the heat flux. If the heat flux is mainly controlled by wind speed, as shown on seasonal and intraseasonal timescales [see C. Wang (1995) and Weisberg and Wang (1997) for observed and analytical results], then the decrease in heat flux due to decreasing wind speed overcomes the increase in heat flux due to increasing moisture content. The net result is a decrease in heat flux, less ocean cooling, and, hence, an increase in SST.

However, for the conventional zonal wind stress–SST feedback the atmosphere interacts dynamically with the ocean through momentum flux. The basis for the conventional zonal wind stress–SST feedback is that increasing equatorial SST decreases equatorial easterly wind stress, which, in turn, further affects the ocean through momentum flux to increase equatorial SST by variations in thermocline depth due to either upwelling or entrainment. This positive feedback can be better explained by the relationship between zonal wind stress and SST gradient (Lindzen and Nigam 1987). Increasing SST in the equatorial central/eastern Pacific decreases zonal SST gradient, which reduces easterly wind stress. Reducing easterly wind stress, in turn, further increases SST in the equatorial central/eastern Pacific by dynamical response. The zonal wind stress–SST feedback appears to operate on interannual timescales (e.g., Philander 1990). In nature, both the zonal wind stress–SST feedback through dynamical response and the wind speed–evaporation–SST feedback through thermodynamical response are likely to be important, each occuring on different timescales.

With the thermodynamical wind speed–evaporation–SST feedback operating on seasonal and intraseasonal timescales and the dynamical zonal wind stress–SST feedback operating on interannual timescales, the interactions between these two different timescale feedback processes can produce irregular oscillations. The key element for the model irregularity demonstrated herein is the annual variability in the wind speed–evaporation–SST feedback. Since the atmosphere adjusts quickly in comparison with the ocean, we can assume that the atmosphere is in equilibrium with the evolving ocean. Thus, Eq. (6) can be further simplified by dropping the time derivative: $U = (f/g)T$. While not shown, this steady atmosphere model produces a similar result as Fig. 3 (using the same parameters). This is not a

surprising result since in both cases zonal wind anomaly is linearly related to the SST anomaly.

From Eq. (5), the inclusion of the latent heat flux process in the delayed oscillator model acts as a cooling effect. That is, the role of the heat flux is to help the delayed negative feedback of the oceanic wave dynamics to bring the system from a warm (cold) state to a cold (warm) state. One must keep in mind that this cooling effect also depends upon the atmospheric wind speed. It is the dependence upon the atmospheric wind speed that forms the actively positive wind speed–evaporation–SST feedback. Mathematically, the term of the wind speed–evaporation–SST feedback $-c|\overline{U} + U|$ in Eq. (5) can be combined with the local positive feedback term aT to get a new local coupling term $a'T$, where $a' = a - c|\overline{U} + U|$. Therefore, an annual cycle of the mean zonal wind in the wind speed–evaporation–SST feedback process is equivalent to an annual cycle in the local coupling coefficient a'. It is anticipated that an annual cycle in the local coupling processes is also able to produce the irregularity of the model oscillations. An experiment in which the local coupling coefficient a has an annual cycle without the latent heat flux process ($c = 0$) confirms this speculation (not shown). The annual cycle in the local coupling process has its own physical basis. Observations show that both surface wind and SST as well as thermocline in the equatorial Pacific vary annually (e.g., Hayes et al. 1991; Weisberg and Wang 1997). Thus, it is not unreasonable to assume that the local coupling coefficient has an annual cycle.

The phase-locking of ENSO to the seasonal cycle depends largely upon how the annual cycle is specified. The model ENSO onset and peak can occur in any calendar month by varying the time of annual cycle in the wind speed–evaporation–SST feedback. In all our experiments, we have specified the annual cycle of mean zonal wind to be consistent with observations. That is, the weakest (strongest) easterly winds occur in the boreal spring (fall). The resulting phase-locking is that the model ENSO onset and peak occur during the boreal winter and spring, respectively, consistent with the observed phase-locking of ENSO in the far eastern Pacific. Since the key for the model phase-locking is the annual cycle in the wind speed–evaporation–SST feedback, it implies that the wind speed–evaporation–SST feedback may mostly occur in the far eastern Pacific. Note that the analogical delayed oscillator has been previously applied to different regions. When Suarez and Schopf (1988) first proposed the delayed oscillator, they argued that the ocean–atmosphere coupling is strongest in the central equatorial Pacific, implying that it is applied there. Battisti and Hirst (1989) later derived the delayed oscillator model, based on the coupled model of Zebiak and Cane (1987), by taking an area average over the region between 160° and 80°W, which includes the far eastern Pacific. Cane et al. (1990) also derived a version of the delayed oscillator model that controls the variation of eastern Pacific boundary thermocline displacement.

The model ENSO peak herein is inconsistent with the observed phase of maximum SST anomalies in the Nino3 region that occurs near the end of the El Niño year. The inconsistency suggests that other processes may contribute to the phase-locking of ENSO in the Nino3 region. By emphasizing different physical processes, many studies have discussed the phase-locking of ENSO to the seasonal cycle in the Nino3 region. The model ENSO peak phases of these studies tend to occur either early (e.g., Chang et al. 1995; Tziperman et al. 1995) or late (Wang and Fang 1996) in comparison with observations, suggesting that the physics for the phase-locking in the Nino3 region are more complicated and that further studies are needed. For example, here we only consider zonal winds whereas meridional winds may also play a role.

Why is the model ENSO phase-locked to the seasonal cycle? In general, when there is an external periodic forcing in a nonchaotic oscillatory system, the oscillatory system will entrain to the external forcing so that the period of the oscillatory system becomes a rational multiple of the forcing period. As a result, the phase of the oscillatory system is, to some extent, locked into the phase of the forcing. As a simple analog, consider a spring attached at one end and free at the other. This system can produce a free oscillatory motion. Now if one places a periodic forcing at the free end, the spring will undergo a transition and entrain its phase so that the phase of the spring is consistent with that of the forcing every integer number of forcing periods. This phenomenon is referred to as phase-locking in the engineering literature (Guckenheimer and Holmes 1983). Therefore, the model ENSO onset and peak will occur only at a particular month of year when the model solution is periodic. Even when the solution is chaotic or quasiperiodic, most of the model ENSO onsets and peaks still occur near a particular month (Figs. 7 and 11).

The route to chaos in this study is the intermittency route, differing from the period doubling of Chang et al. (1995) and the quasiperiodicity of Tziperman et al. (1995). This suggests that the transition to chaos of ENSO models as a parameter is increased can occur in any of three universally recognized standard scenarios. The difference may be manifestations of different approaches by using different models. However, all these models showed that annual cycle forcing is critical for the chaotic oscillations. The similarity implies that the interactions between the annual and interannual cycles is a robust mechanism of generating the irregularity of ENSO.

Gu and Philander (1997) recently proposed that the influx of water from higher latitudes induces interdecadal climate variability. The influx following surfaces of constant density, which rise from the tropical thermocline to the ocean surface in the extratropics, affects

equatorial SST by a delay term and, hence, the tropical and extratropical winds that in turn affect the influx. Such processes give rise to continual interdecadal oscillations. The simple model herein shows that decadal or interdecadal climate variability is also possible when considering the Tropics only. The mechanism for such decadal or interdecadal variability is the nonlinear interactions between the annual and interannual cycles. In a linear system, the summation of two high-frequency oscillations will produce a lower-frequency wave packet oscillation. The wave packet frequency is the frequency difference between two high frequencies. Inclusion of nonlinearity results in further modulation of the wave packet. The model SST anomaly in Fig. 8d shows that the decadal variability looks like a wave packet. In fact, the coupled tropical ocean–atmosphere system, itself inducing decadal or interdecadal variability, is also shown in more complicated models although the mechanism has not been studied [see Latif (1998) for review]. Both the mechansim of Gu and Philander (1997) and that of the nonlinear interactions between the annual and interannual cycles proposed herein for decadal or interdecadal variability may be operant in nature.

The analogical model herein, considering both ocean dynamics and thermodynamics, provides a possible explanation for irregularity and phase-locking of ENSO. However, more realistic coupled GCMs or intermediate coupled models including the wind speed–evaporation–SST feedback are necessary to investigate whether such dynamical and thermodynamical interactions are representative of ENSO. Many other hypotheses have also been developed for the irregularity of ENSO. For example, Graham and White (1988) attributed irregularity to the random forcing of the ocean–atmosphere system. Munnich et al. (1991) have examined a simplified, nonlinear ocean–atmosphere model and found that irregular interannual variability can result from the coupling between the ocean and the atmosphere even in the absence of seasonal forcing. Vallis (1986, 1988) argued that the irregularity of ENSO arises naturally and deterministically within a simple framework, without stochastic, seasonally varying forcing and without ocean wave dynamics. Given such widely differing hypotheses for irregularity of ENSO, further studies are necessary on this important topic.

Acknowledgments. This study was supported by the NOAA Office of Global Programs under Global Ocean–Atmosphere–Land System (GOALS) Program Grant NA66GPO119. We thank the anonymous reviewers for their helpful comments on the earlier draft. Mr. E. Siegel helped prepare three of the final figures.

REFERENCES

Battisti, D. S., and A. C. Hirst, 1989: Interannual variability in the tropical atmosphere–ocean model: Influence of the basic state, ocean geometry and nonlineary. *J. Atmos. Sci.,* **46,** 1687–1712.

Cane, M. A., M. Munnich, and S. E. Zebiak, 1990: A study of self-excited oscillations of the tropical ocean–atmosphere system. Part I: Linear analysis. *J. Atmos. Sci.,* **47,** 1562–1577.

Chang, P., B. Wang, T. Li, and L. Ji, 1994: Interaction between the seasonal cycle and ENSO frequency entrainment and chaos in a coupled atmosphere-ocean model. *Geophys. Res. Lett.,* **21,** 2817–2820.

——, L. Ji, B. Wang, and T. Li, 1995: Interactions between the seasonal cycle and El Niño–Southern Oscillation in an intermediate coupled ocean–atmosphere model. *J. Atmos. Sci.,* **52,** 2353–2372.

Graham, N. E., and W. B. White, 1988: The El Nino cycle: A natural oscillator of the Pacific Ocean-atmosphere system. *Science,* **240,** 1293–1302.

Gu, D., and S. G. H. Philander, 1997: Interdecadal climate fluctuations that depend on exchanges between the tropics and extratropics. *Science,* **275,** 805–807.

Guckenheimer, J., and P. Holmes, 1983: *Nonlinear Oscillations, Dynamical Systems, and Bifurcations of Vector Fields.* Springer-Verlag, 459 pp.

Hayes, S. P., P. Chang, and M. McPhaden, 1991: Variability of the sea surface temperature in the eastern equatorial Pacific during 1986–1988. *J. Geophys. Res.,* **96,** 10 553–10 566.

Jin, F.-F., J. D. Neelin, and M. Ghil, 1994: El Nino on the Devil's Staircase: Annual subharmonic steps to chaos. *Science,* **264,** 70–72.

Latif, M., 1998: Dynamics of interdecadal variability in coupled ocean–atmosphere models. *J. Climate,* **11,** 602–624.

——, and T. P. Barnett, 1995: Interactions of the tropical oceans. *J. Climate,* **8,** 952–964.

Lindzen, R. S., and S. Nigam, 1987: On the role of sea surface temperature gradients in forcing low-level winds and convergence in the tropics. *J. Atmos. Sci.,* **44,** 2418–2436.

Lorenz, E. N., 1963: Deterministic nonperiodic flow. *J. Atmos. Sci.,* **20,** 130–141.

McCreary, J. P., and D. L. T. Anderson, 1991: An overview of coupled ocean-atmosphere models of El Nino and the Southern Oscillation. *J. Geophys. Res.,* **96,** 3125–3150.

Munnich, M., M. Cane, and S. E. Zebiak, 1991: A study of self-excited oscillations of the tropical ocean–atmosphere system. Part II: Nonlinear cases. *J. Atmos. Sci.,* **48,** 1238–1248.

Oberhuber, J. M., 1988: An atlas based on the COADS data set: The budget of heat, buoyancy and turbulent kinetic energy at the surface of the global ocean. Max-Planck Institut für Meteorologie, Rep. 15, 199 pp. [Available from Max-Planck Institut für Meteorologie, Bundesstrasse 55, 2000 Hamburg 13, Germany.]

Philander, S. G., 1990: *El Nino, La Nina, and the Southern Oscillation.* Academic Press, 289 pp.

Rasmusson, E. M., and T. H. Carpenter, 1982: Variations in tropical sea surface temperature and surface wind fields associated with the Southern Oscillation/El Niño. *Mon. Wea. Rev.,* **110,** 354–384.

Suarez, M. J., and P. S. Schopf, 1988: A delayed action oscillator for ENSO. *J. Atmos. Sci.,* **45,** 3283–3287.

Tziperman, E., L. Stone, M. Cane, and H. Jarosh, 1994: El Nino chaos: Overlapping of resonances between the seasonal cycle and the Pacific Ocean-atmosphere oscillator. *Science,* **264,** 72–74.

——, M. Cane, and S. E. Zebiak, 1995: Irregularity and locking to the seasonal cycle in the ENSO prediction model as explained by the quasi-periodicity route to chaos. *J. Atmos. Sci.,* **52,** 293–306.

Vallis, G. K., 1986: El Niño: A chaotic dynamical system? *Science,* **232,** 243–245.

——, 1988: Conceptual models of El Niño and Southern Oscillations. *J. Geophys. Res.,* **93** (C), 13 979–13 991.

Wang, B., 1995: Interdecadal changes in El Niño onset in the last four decades. *J. Climate,* **8,** 267–285.

——, and Z. Fang, 1996: Chaotic oscillation of tropical climate: A

dynamical system theory for ENSO. *J. Atmos. Sci.*, **53,** 2786–2802.

Wang, C., 1995: Numerical, analytical, and observational studies of tropical ocean-atmosphere interactions. Ph.D. dissertation, University of South Florida, 184 pp. [Available from University of South Florida, 140 7th Ave. S., St. Petersburg, FL 33701.]

Weisberg, R. H., and C. Wang, 1997: Slow variability in the equatorial west-central Pacific in relation to ENSO. *J. Climate,* **10,** 1998–2017.

Wolf, A., J. B. Swift, H. L. Swinney, and J. A. Vastano, 1985: Determining Lyapunov exponents from a time series. *Physica D,* **16,** 285–317.

Xie, S.-P., 1996: Westward propagation of latitudinal asymmetry in a coupled oceans–atmosphere model. *J. Atmos. Sci.*, **53,** 3236–3250.

——, and S. G. Philander, 1994: A coupled ocean-atmosphere model of relevance to the ITCZ in the eastern Pacific. *Tellus,* **46A,** 340–350.

Zebiak, S. E., and M. A. Cane, 1987: A model El Niño–Southern Oscillation. *Mon. Wea. Rev.*, **115,** 2262–2278.